Multi-Phase Fracture-Matrix Interactions Under Stress Changes

Technical Progress Report
Semi-Annual

Reporting Period
September 21, 2001 – March 20, 2002

Principal Authors:

A. S. Grader, D. Elsworth, P. M. Halleck, F. Alvarad,
H. Yasuhara, A. Alajmi

Report issue Date: 4/20/2002

DOE Award Number: DE-FC26-01BC15355

Submitting Organization:

A. S. Grader
203 Hosler Building
The Energy Institute
The Penn State University
University Park, PA 16802

DISCLAIMER

ABSTRACT

The main objectives of this project are to quantify the changes in fracture porosity and multi-phase transport properties as a function of confining stress. These changes will be integrated into conceptual and numerical models that will improve our ability to predict and optimize fluid transport in fractured system. This report details our progress on **a**. *developing the direct experimental measurements of fracture aperture and topology using high-resolution x-ray micro-tomography,* **b**. *modeling of fracture permeability in the presence of asperities and confining stress*, and **c**. *simulation of two-phase fluid flow in a fracture and a layered matrix*.

The three-dimensional surface that describes the large-scale structure of the fracture in the porous medium can be determined using x-ray micro-tomography with significant accuracy. The distribution of fracture aperture is a difficult issue that we are studying and developing methods of quantification. The difficulties are both numerical and conceptual. Numerically, the three-dimensional data sets include millions, and sometimes, billions of points, and pose a computational challenge. The conceptual difficulties derive from the rough nature of the fracture surfaces, and the heterogeneous nature of the rock matrix. However, the high-resolution obtained by the imaging system provides us a much needed measuring environment on rock samples that are subjected to simultaneous fluid flow and confining stress.

The absolute permeability of a fracture depends on the behavior of the asperities that keep it open. A model is being developed that predicts the permeability and average

aperture of a fracture as a function of time under steady flow of water including the pressure solution at the asperity contact points.

Several two-phase flow experiments in the presence of a fracture tip were performed in the past. At the present time, we are developing an inverse process using a simulation model to understand the fluid flow patterns in the presence of a fracture, and the interactions between fluid flow in the fracture and the adjacent matrix. Preliminary results demonstrate that the flow patterns are significantly impacted by the presence of the fracture. Bypassing is quantified and we expect to be able to extract from the modeling the distribution of properties in the fracture and the adjacent matrix.

TABLE OF CONTENTS

LIST OF FIGURES

INTRODUCTION

Natural and artificially-induced fractures in a reservoir have a great impact on fluid flow patterns and on the ability to recover hydrocarbons. In tight formations, the naturally fractured system provides access to the hydrocarbon fluids stored in the matrix. Fractures can have a negative effect on recovery processes when they form bypassing paths, especially in production-injection systems. For example, injected fluid may preferentially flow through the fractures leaving behind inaccessible and non-contacted hydrocarbons. Fractures can enhance the efficiency of displacement operations when the main direction of flow is perpendicular to the direction of the fractures. Fractures may also be non-conductive and form barriers to fluid flow. The mass transport between the fractures and the surrounding matrix has an important role in being able to predict and optimize the recovery processes from fractured reservoirs. As production occurs and pore pressures decline, the net confining stress on the rock increases. This project focuses on the effects that changes in confining stress have on the transport properties of the fracture-matrix system. The confining stress has an impact on the fracture aperture and therefore on multiphase fluid transport properties (*Barton et al.*, 1985, *Gentier et al.*, 1997). We propose to quantify the changes in fracture porosity and saturation distribution under steady and non-steady flow in both the fracture and the adjoining matrix. The quantitative changes will be obtained by low and high resolution X-ray computerized tomography (CT) imaging (*Vinegar and Wellington*, 1987), and then these changes will be used in an inverse simulation process to quantify changes in permeabilities and to suggest up-scaling procedures.

We propose a fracture-matrix interaction program with the following objectives:

• Quantify the effects of confining stress on fracture topology and aperture and porosity.

• Quantify the changes in two-phase fracture permeabilities as a function of stress.

• Determine the effect of stress on oil-water transport between the fracture and the matrix.

• Determine the effects of stress on recovery processes in the presence of fractures.

• Use inverse simulation of four-dimensional saturation data for up-scaling.

We approach multi-phase flow in stressed fractured rocks experimentally and computationally. We will use multi-phase injection into confined rock samples that contain natural fractures or artificially induced ones. We will quantify the saturation distribution temporally and spatially (four-dimensional) using our new imaging facility and The Center for Quantitative Imaging. We will also monitor the pressure behavior of the sample and confining fluids. The resulting four-dimensional distribution of saturations and pressure histories will form the basis for multi-phase fluid flow simulation with the ultimate goal of quantifying the changes in the fluid flow characteristics of the rock as a function of the net confining stress. This combined experimental/computational approach will lead to advances in our understanding of the effects in-situ stress on recovery processes.

EXECUTIVE SUMMARY

The main objectives of this project are to quantify the changes in fracture porosity and multi-phase transport properties as a function of confining stress. These changes will be integrated into conceptual and numerical models that will improve our ability to predict and optimize fluid transport in fractured system. The project has five tasks:

1. Quantify the effects of confining stress on fracture topology and aperture and porosity.
2. Quantify the changes in two-phase fracture permeabilities as a function of stress.
3. Determine effects of stress on oil-water transport between the fracture and the matrix.
4. Determine the effects of stress on recovery processes in the presence of fractures.
5. Use inverse simulation of four-dimensional saturation data for up-scaling.

This report focuses mainly on tasks 1, 3, and 5.

Fracture Topology and Aperture: Several high-resolution x-ray CT data sets were acquired using layered sand stones and chalk that were artificially fractured in tension. The analysis focused on characterizing the overall topology of the fracture and the distribution of its aperture, or fracture width. Two examples are presented in the report. The topology of the fracture in chalk is more variable than in the layered Berea sand stone. The fracture in the sandstone was created in a perpendicular orientation to the layers. Previous fluid displacement in the fracture yielded observations of high permeability adjacent to high permeability layers. This observation is confirmed by analysis presented in this report. The fracture aperture map resembles the layer map of the sample. We plan to confirm this observation as well as to verify the aperture calculations using destructive methods.

Modeling of Fracture Closure: There is much literature treating a fracture as a gap between two parallel plates. We have been of the opinion that most fractures are far from such a description, and have rough walls with asperities that maintain keep the fracture from closing. Also, the fracture topology is not a single plane, and has significant variations. We are in the early stages of developing a model that can describe the effective fracture aperture, and thus fracture permeability, as a function of time under various histories of confining pressure, temperature, and the rate of water flow. We observe that increasing the temperature accelerates the pressure solution of the asperities and allows the fracture to close and reduce the absolute permeability.

Modeling of Fracture-Matrix Fluid Flow Interactions: Some previously performed two-phase flow experiments are being analyzed. In one of these experiments, a layered sample was fractured at the inlet end, with an axial fracture that extended only to the middle of the sample, creating a fracture tip. The oil loading process is being modeled. Preliminary results allow us to understand the oil and water flow patterns. As oil is injected, most of it flows through the fracture until it reaches the fracture tip. Then it diverges through the layers to form a stable displacement through the entire cross-section of the sample. Contrary to initial analysis, the bypassed water in the part of the matrix adjacent to the fracture flows forward and away from the fracture to the outer regions of the core and not to the fracture. This simulation observation is assisting in designing tracer tests to confirm the simulation results. Three-dimensional inverse simulation to determine permeabilities and capillary pressures are the ultimate goal of this task.

EXPERIMENTAL SYSTEM

The experimental system used in this project includes a multi-phase fluid flow system, a core holder assembly that can provide controlled confining pressure, and an x-ray computed tomography system. A schematic of the system is shown in Figure 1 and photographs of the medical and the industrial scanners are shown in Figure 2. Since the program is in its early stages, the focus in this report is on the high-resolution x-ray imager. Most of the details of the fluid flow system can be found in *Alajmi and Grader* (2000).

The images consist of an ionized x-ray source, a detector, a translation system, and a computer system that controls motions and data acquisition. The x-ray source has a Tungsten target with a focal spot of 5 microns. It produces a cone beam that passes through the core and activates the detector. The image intensifier detector surface releases electrons that are then focused on a screen that is photographed by a high-resolution (1024x1024) camera with a frequency of 15 Hz. The sample is rotated 360 degrees in the x-ray beam while the detector is providing attenuation views to the data acquisition computer. After the sample is rotated a complete turn, the system reconstructs a slice, a cross-sectional image of the attenuation values that represents a combination of the density and the apparent atomic number of the sample and the imaged position. The imager operates in volume mode where several separate slices are collected in one rotation. In the example shown in the report, up to 41 slices were acquired in a

single rotation. After each rotation, the sample is translated axially to a new scanning position, thus, allowing a continuous three-dimensional coverage of the sample.

Fluids are introduced to the sample through pipes that are able to sustain the rotation and the translation of the sample. There are two fluid injection line, one fluid production line, one confining pressure line, and two pressure measurement lines. All of fluid connections are compatible with the x-ray system. Three rock samples are reported in this report. They include a two Berea sandstone samples and a chalk sample. These samples were fractured artificially using a modified Brazilian test. In classical rock mechanics this test is used on thin disc loaded by uniform pressure that is applied radially over a short strip of the circumference at each end of the diameter. The underlying hypothesis of the Brazilian test is that the fracture starts from the center of the disc where, assuming that the material is homogeneous, isotropic and linearly elastic. In our case, we applied the pressure over 15 centimeters of the sample, thus creating a long fracture. A photograph of a sample in the stress frame and a photograph of the fractured sample are shown in Figure 3. Details of the fracturing method are given by *Grader et al.* 2000.

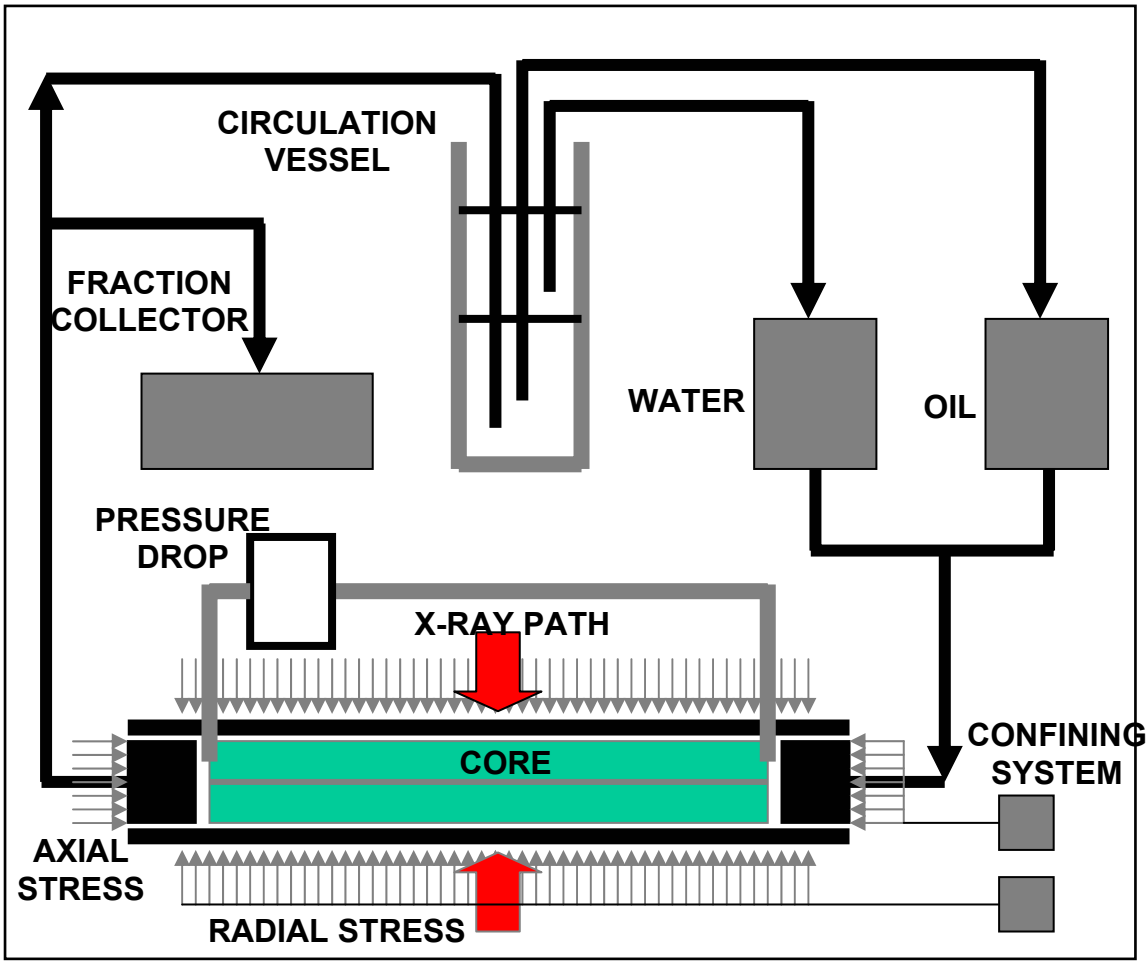

Figure 1: A schematic diagram of the fluid flow and rock sample apparatus.

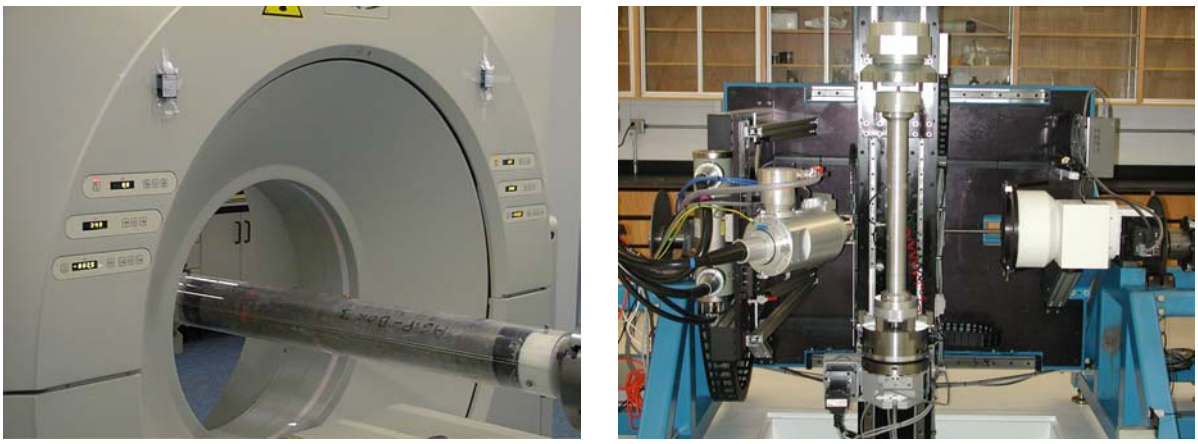

Figure 2: A uni-axial core holder positioned in the medical scanner (left, horizontal) and the industrial scanner (right, vertical).

Figure 3: A Layered Berea rock being fracture using the modified Brazilian procedure. Sample diameter is 50 mm. The photograph below shows the sample with the axial fracture.

RESULTS AND DISCUSSION

Fracture Topology and Aperture:

Fracture aperture and its spatial geometry are key parameters in determining multi-phase fluid transport. The advent of high-resolution Computed Tomography x-ray imaging, CT, provides the opportunity to estimate these geometrical fracture properties in a non-destructive fashion. Two fractured sandstone samples and one chalk sample have been scanned under dry conditions and analysis methods are being developed. Figure 4 presents an example of each sample. Figure 4(a) shows an artificial fracture in a strongly layered Berea sample and Figure 4(b) has layers with reduced contrast. Figure 4(c) is an

image of a chalk sample showing a natural fracture as the white linear feature, and with artificially induced fractures in black. These samples have a diameter of about 50 mm and the pixel resolution is 50 microns in three dimensions. The images shown here are part of a large number of images that cover a three-dimensional volume of each sample. Figure 5 shows a three-dimensional rendering of the fractures in the chalk sample. The fractures were isolated numerically from the CT data and displayed as three-dimensional objects. The figure demonstrates our ability to extract the fracture from the CT data. Methods for quantifying the distribution of fracture apertures and the topography of the fractures are being developed.

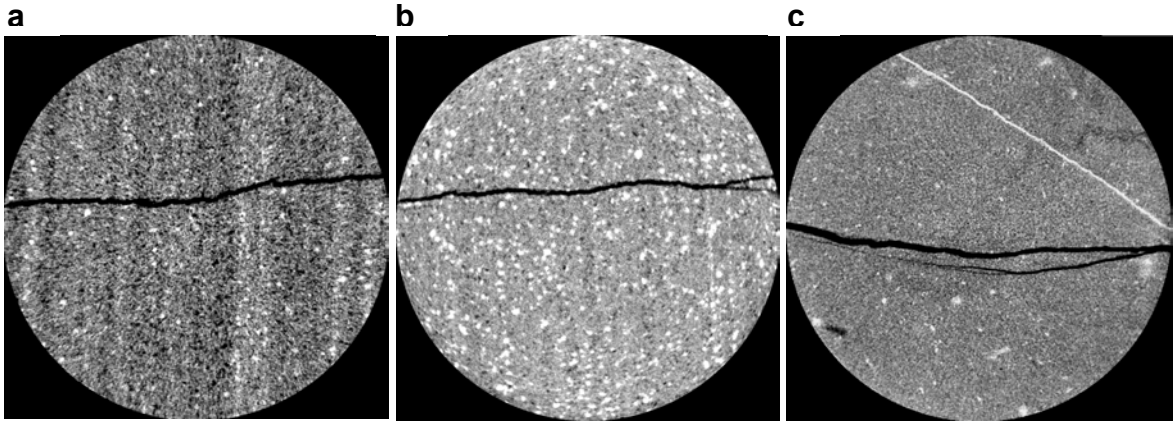

Figure 4: Sample images of fractured samples: a: Berea with strong layering. b: Berea with weak layering. c: Chalk with natural and induced fractures.

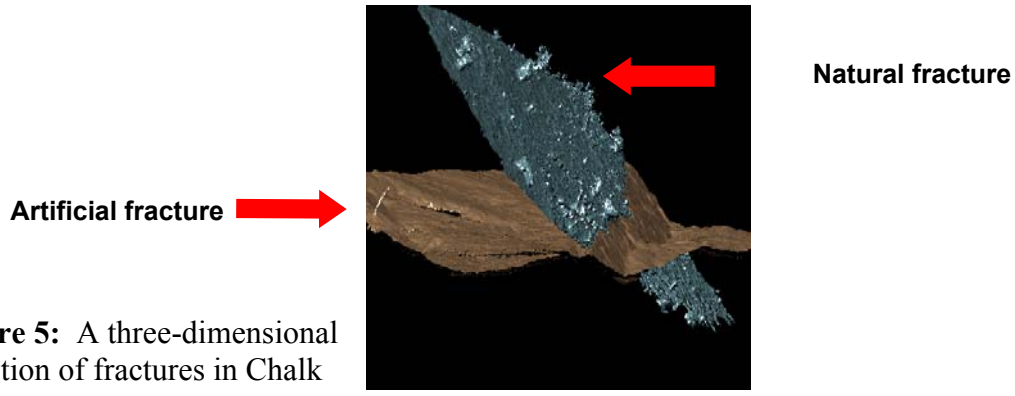

Figure 5: A three-dimensional rendition of fractures in Chalk

The Berea sample (b) was also scanned in the medical scanner in order to compare the ability to extract the resolution of the fracture topology.

The inlet portion of the Berea sample shown in Figure 1a was scanned with the high resolution scanner. A total of 1220 slices at a matrix size of 1024x1024 were acquired (more than a billion points). Using thresholding and dilating methods, the fracture was isolated, and a preliminary distribution of the fracture was isolated. Figure 6 shows a three-dimensional view of the fracture in the Berea sample shown in Figure 1a. The large black spots shown on the surface of the fracture represents closed portions of the fracture, or large asperity regions. These areas located in a specific region of the fracture, and the significance of this location is still unclear. However, these areas have reduced permeability caused by a diminishing fracture width.

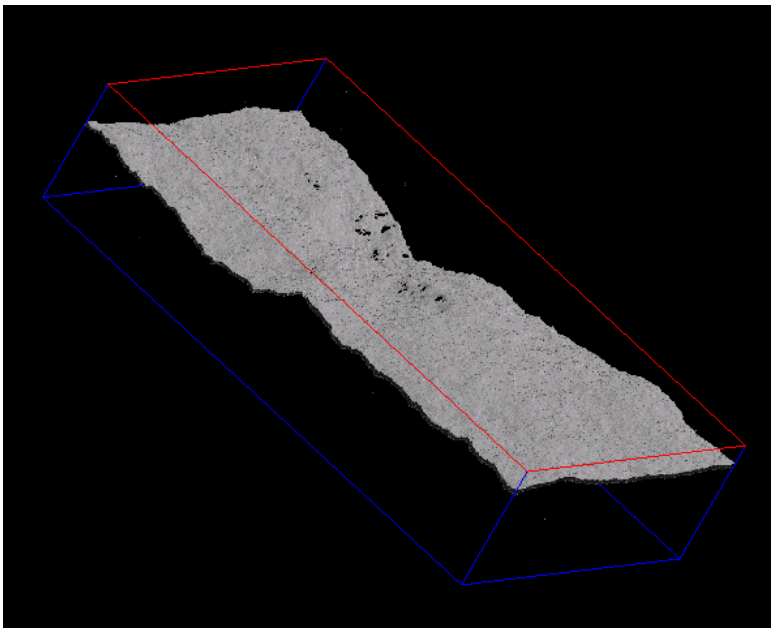

Figure 6: A three-dimensional rendition of a fracture in a layered Berea sample.

After the fracture was isolated numerically in each of the 1220 images, its vertical width (considering that the fracture was oriented in a horizontal fashion) was computed at every

horizontal position. The two-dimensional view of fracture width is shown in Figure 7a. The white line represents one CT slice that a portion of it is shown in Figure 8, just below the trimmed map of the with in Figure 1b. The scale of the width ranges from 0 (black) to 1000 microns (white). The average fracture with over the entire region covered in Figure 7 was 540 microns. Figures 7b and 8 demonstrate that there is a strong correlation between fracture width and the porosity of the adjoining layers. The low porosity adjoining layers in Figure 8 are denoted by the light gray color, and they correspond to the dark stripes in Figure 7b that represents small fracture widths.

The spatial structure of the fracture and its width distribution provides us the physical layout for numerical modeling of fluid flow in the fracture and the interaction with the matrix.

7a

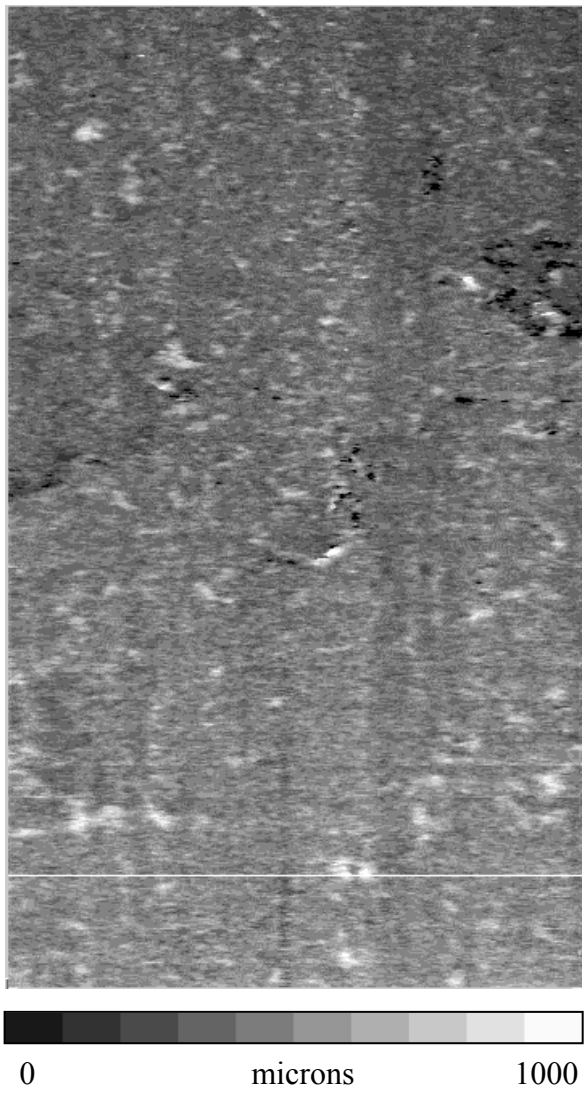

Figure 7: A map of distribution of fracture Width. 7a: The entire portion of the fracture (61 mm x 35 mm). 7b: The upper portion of Figure 7a, up to the selected image shown in Figure 8

7b

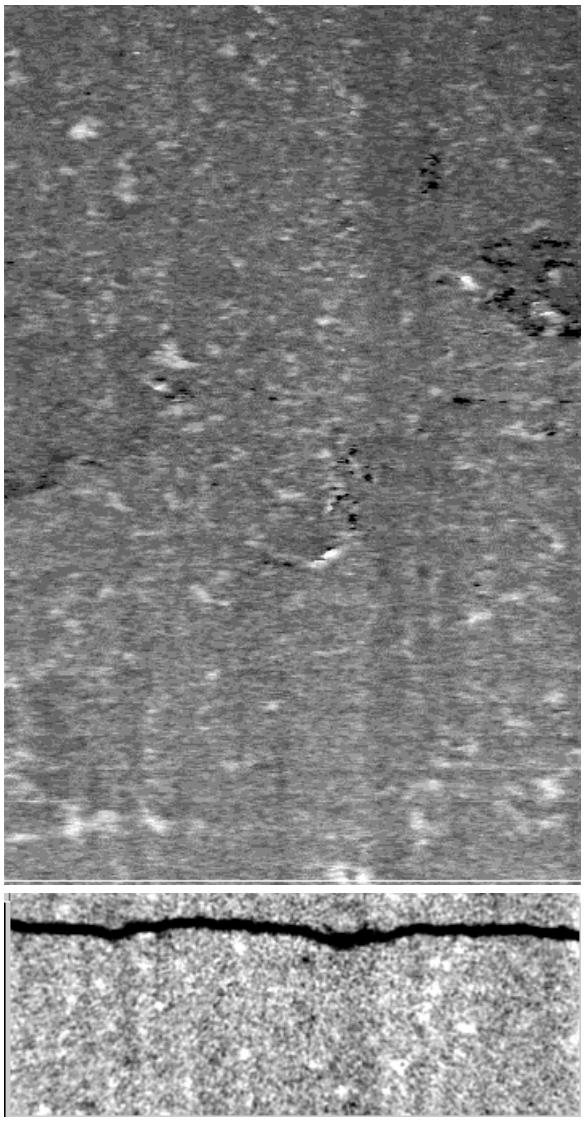

Figure 8: A selected portion of an image highlighted as the white horizontal line on Figure 7a.

Figure 9 shows a comparison between the medical scanner (left) and the OMNI-X industrial micro-tomography scanner (right). The superior resolution of the industrial scanner is demonstrated. However, more work is needed to determine under what

conditions are the medical data sufficient. In the presented figure, the medical voxel size is 0.25x0.25x2 mm. The industrial image has a voxel resolution of 0.05x0.05x0.05 mm. The industrial imager produces images with an improved resolution over the medical scanner by about three orders of magnitude. The high-resolution three-dimensional data provide the ability to significantly narrow the uncertainty associated with estimating the distribution of fracture topology and the distribution of fracture apertures.

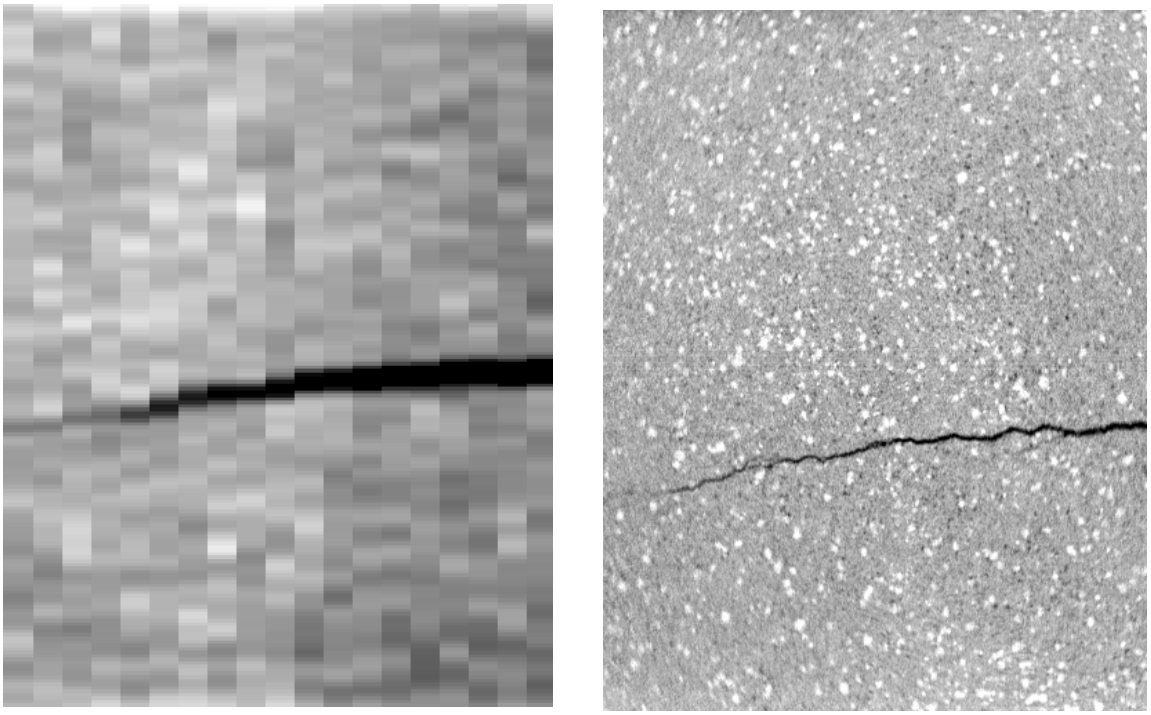

Figure 9: A comparison between axial reconstructions along a fracture. Left: medical. Right: industrial micro-tomography.

Modeling of Fracture Closure:

Work has begun to evaluate the changes in permeability that result from the application of normal stress to a fracture. The fracture is idealized as two rough surfaces in contact. The initial approach is to treat the contacting asperities as viscous contacts (Revil 1999, 2001) that will deform plastically in response to applied load, as illustrated schematically

in Figure 10. Closure of the fracture will progress until an equilibrium contact stress is attained where the high contact stresses are reduced to a level that plastic deformation will not occur. This gives the asymptotic closure of the fracture, and enables the effective parallel plate permeability to be evaluated. The rate at which closure progresses is controlled by the deformation rate present at the contacting asperities. This rate is controlled by the effective viscosity of the deformation contacts, and is controlled by the effective rates of dissolution and diffusion at the asperity contact locations. This behavior is represented in the figure as local asperity stresses, σ_c, reduces as the load is spread over an increasing contact area, A_c. This reduces the local stress driving the viscous compression, and the rate of closure slows, as evident in the plot of fracture aperture with time under constant applied stress, in Figure 11.

The equilibrium contact area is defined by both the equilibrium contact stress, σ_c, that is in turn defined by the energy of the mineral surfaces in contact, and the average applied stress, σ. Where the system temperature, the temperature of fusion of the mineral surfaces, and the heat of fusion of the mineral surfaces are known, together with the fracture topography, the equilibrium closure aperture may be evaluated. The rate of progress to this closure may be evaluated from knowledge of dissolution, diffusion, or precipitation rates of the mineral matter, proximal to the asperity contacts. Where diffusion dominates, the rate of diffusion is controlled by both the aqueous diffusion rate and the asperity contact area. This enables the rate of closure to be determined from fracture surface profile data and physical properties. The change in aperture with time

may be evaluated, as illustrated in Figure 11a, and this converted to an equivalent permeability as shown in Figure 11b.

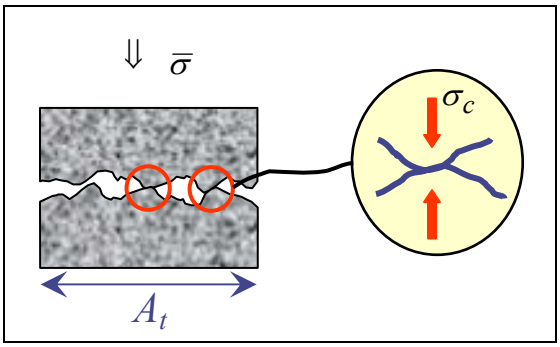

Figure 10: Schematic of the fracture aperture model including asperities.

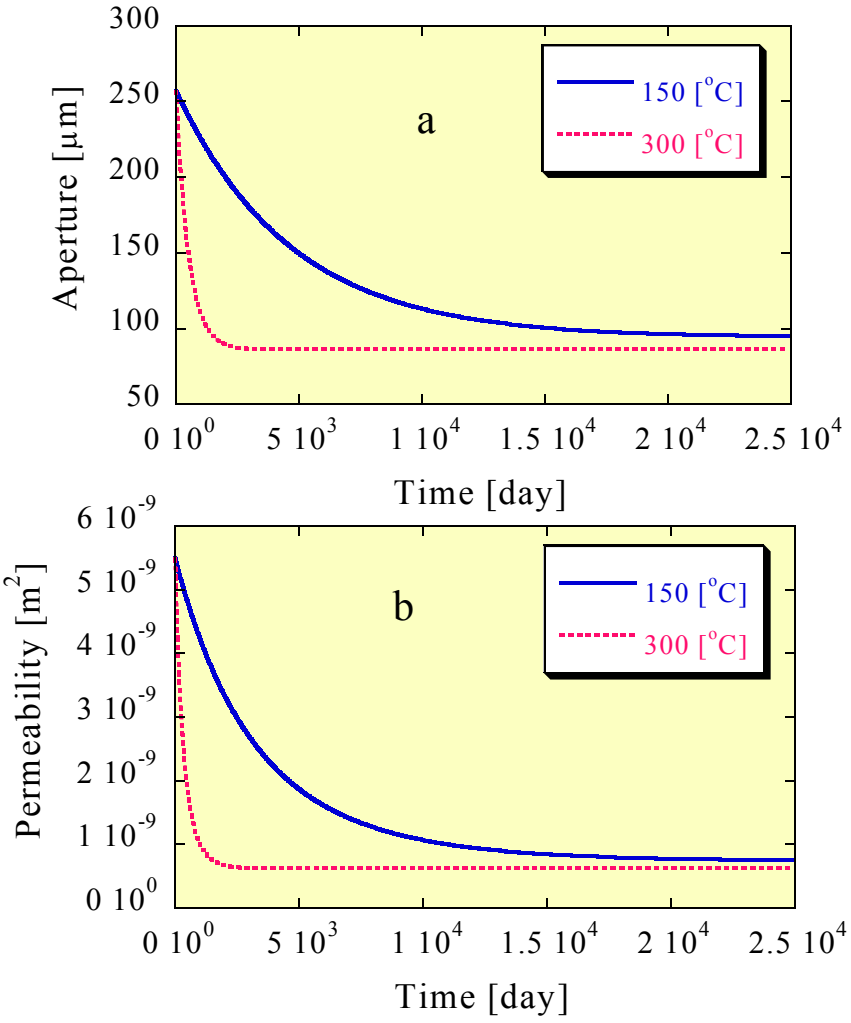

Figure 11: Aperture and Permeability variation with time. a: Aperture. b: Permeability.

Modeling of Fracture-Matrix Fluid Flow Interactions:

The presence of fractures has a significant impact on fluid flow in a porous medium. Two-phase flow experiments are being analyzed in order to understand the flow patterns that develop in the presence of a single fracture in a layered core. The inverse process includes using a numerical fluid flow simulator (Eclipse) to match experimental observations made with x-ray CT. In previous experiments (*Alajmi and Grader*, 2000) a Berea sandstone sample was fractured at one end using the modified Brazilian procedure. The fracture was axial and perpendicular to the layers in the sample. The sample was flooded with water, followed by oil flooding for loading, and finally flooded by water. The entire process was followed by scanning the sample in the medical scanner. Figure 12a shows a single slice through a layered Berea sample prior to inducing a fracture and the fractured sample is shown in Figure 12b. Figure 13 shows an axial reconstruction of the sample that was 610 mm long with a diameter of 51 mm.

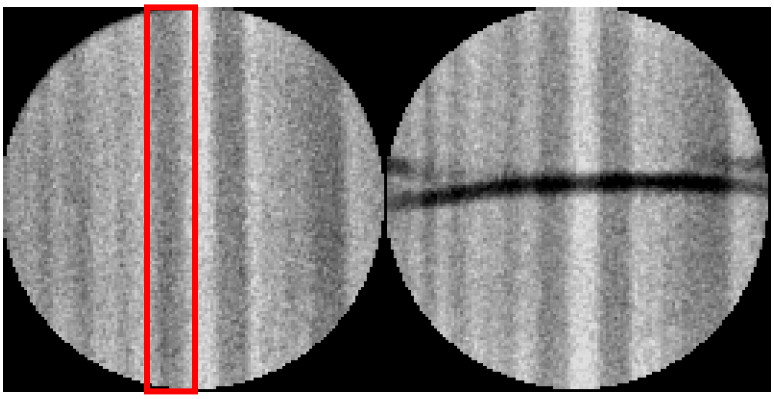

Figure 12: Images of a Berea sample. a: Prior to fracturing. b: Post fracturing.

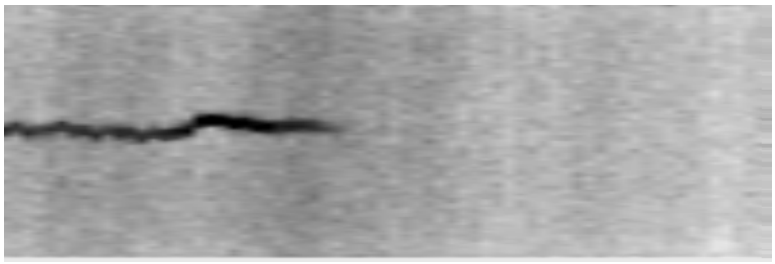

Figure 13: An axial reconstruction of the Berea sample through a single layer.

The CT data were processed to produce a porosity distribution for the entire sample. A single high permeability layer (highlighted in Figure 11a) was selected for initial two-dimensional modeling of fluid flow processes. The sample was saturated with water, oil flooded, and then water flooded. Modeling of the oil flood is the first modeling stage outlined in this report. Using a reservoir simulator and an optimization method, the displacement of water by oil was simulated. Figure 14 shows initial results of average saturation in a single layer along the sample at three different flooding stages. Figure 15 shows the experimental saturation distribution in the sample at the corresponding flood stages. The presence of the fracture creates a bypassing path for the oil, and a significant region adjacent to the fracture remains with high water saturations for an extended period of time. The flow directions of oil and water at a specific flooding stage derived from numerical simulation are shown in figures 16 and 17, respectively. The two-dimensional modeling will provide constraints on the various parameters and simplify three-dimensional modeling.

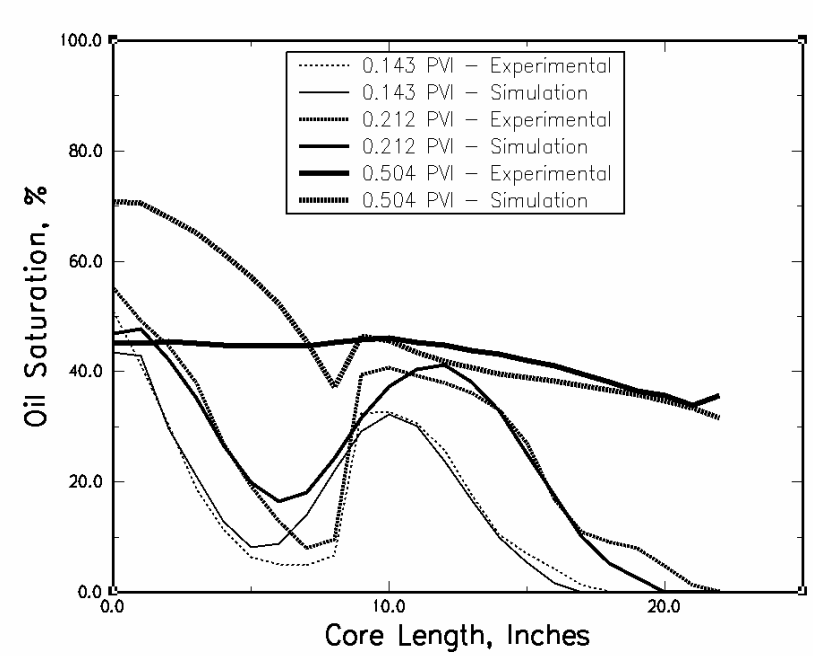

Figure 14: Oil saturation profiles along the core at three different values of Pore Volumes Injected. The profiles demonstrate the effect of the fracture on the displacement process.

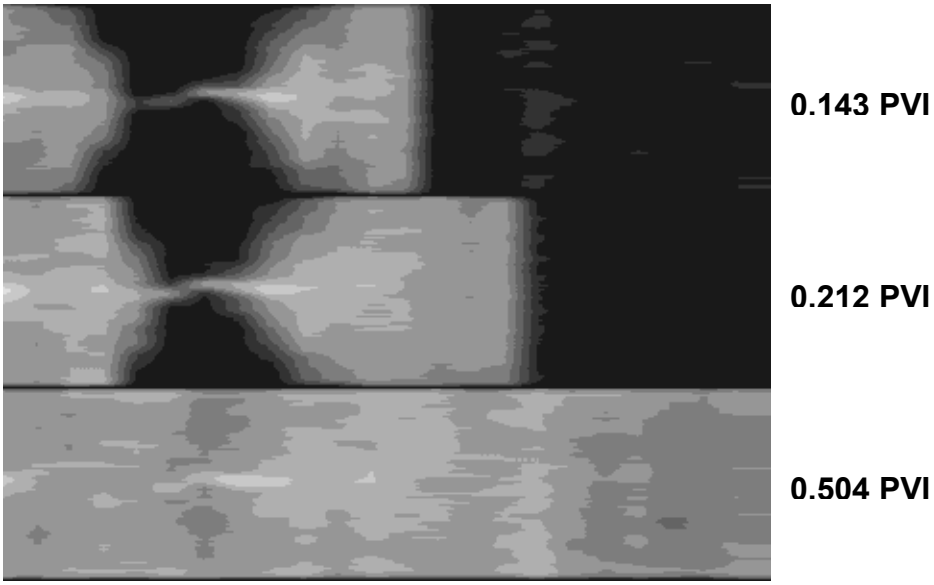

Figure 15: Axial CT reconstructions at three different values of pore volumes injected. The Light shades represent the presence of the injected oil.

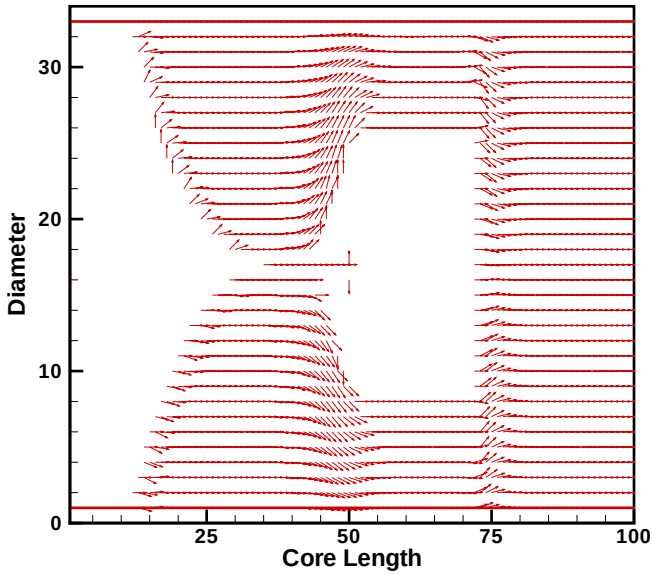

Figure 16: Flow directions and magnitude of water during oil loading of the sample in a single layer prior to breakthrough.

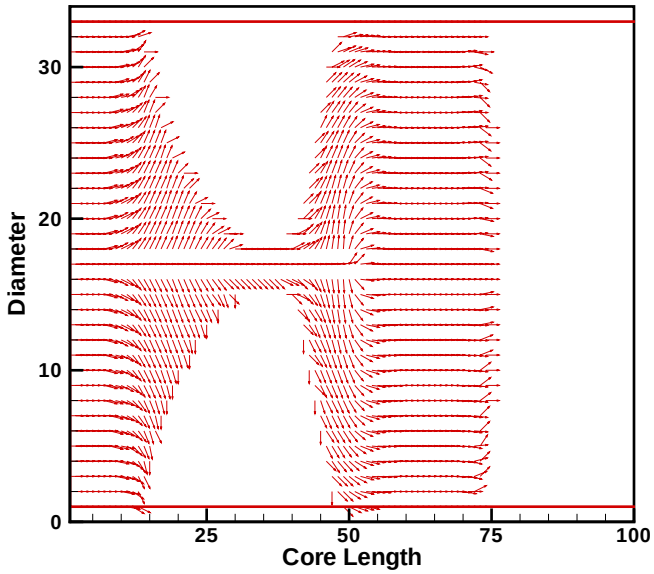

Figure 17: Flow directions and magnitude of oil during oil loading of the sample in a single layer prior to breakthrough.

REFERENCES

Alajmi A., and Grader, A. S., Analysis of Fracture-Matrix Fluid Flow Interactions Using X- Ray CT. Proceedings of The SPE Eastern Regional Conference, Morgantown, West Virginia, 17-19 October 2000.

Barton, N., S. Bandis and K. Bakhtar, Strength, deformation and conductivity coupling of rock joints. *Int. J. R. Mech*., 22, 121 - 140, 1985

.

Gentier, S., and Hopkins, D., (1997) Mapping fracture aperture as a function of normal stress using a combination of casting, image analysis and modeling techniques, Int. J. Rock Mech. & Min. Sci. 34:3-4, Paper No. 132.

Grader, A. S., Balzarini, M., Radaelli, F., Capasso, G., and Pellegrino, A., Fracture-Matrix Flow: Quantification and Visualization Using X-ray Computerized Tomography. AGU Monograph Volume 122, October 2000.

Revil, A. Pervasive pressure solution in a quartz sand. J. Geophys. Res., 106, B5, 8665-8686, 2001.

Vinegar, H. J., and Wellington, S. L., Tomographic Imaging of Three-Phase Flow Experiments, Rev. Sci. Insts., January, pp. 96-107, 1987.

Vukuturi, V. S., Lama, R. D., and Saluja, S. S., Handbook on Mechanics Properties of Rocks, Volume I Trans Tech Publications, 1974.

LIST OF ACRONYMS AND ABBREVIATIONS